Published in final edited form as:
Mol Imaging Biol. 2013 October ; 15(5): 606–613. doi:10.1007/s11307-013-0627-x.

Effects of Chelator Modifications on ^{68}Ga-Labeled [Tyr^3]Octreotide Conjugates

Mai Lin, **Michael J. Welch**, and **Suzanne E. Lapi**
Mallinckrodt Institute of Radiology, Washington University School of Medicine, Campus Box. 8225, 510 South Kingshighway Blvd, St. Louis, MO 63110, USA

Abstract

Purpose—Somatostatin receptors (SSTR) have been reported as promising targets for imaging agents for cancer. Recently, ^{68}Ga-DOTATOC-based PET imaging has been used successfully for diagnosis and management of SSTR-expressing tumors. The purpose of this study was to evaluate the influence of chelator modifications and charge on ^{68}Ga-labeled peptide conjugates.

Procedures—We have synthesized a series of [Tyr^3]octreotide conjugates that consisted of different NOTA-based chelators with two to five carboxylate moieties, and compared our results with ^{68}Ga-DOTATOC in both *in vitro* and *in vivo* studies.

Results—With the exception of ^{68}Ga-**1** (three carboxylates), the increased number of carboxylates on the NOTA-based chelators resulted in a reduced binding affinity and internalization. Additionally, the tumor uptake for ^{68}Ga-**2** (four carboxylates) and ^{68}Ga-**3** (five carboxylates) was reduced compared to that of ^{68}Ga-DOTATOC (three carboxylates) and ^{68}Ga-NO2ATOC (two carboxylates) and ^{68}Ga-**1** (three carboxylates) at 2 h p.i. suggesting the presence of an optimal charge for this compound.

Conclusions—Chelator modifications can lead to the altered pharmacokinetics. These results may impact further design considerations for peptide-based imaging agents.

Keywords

^{68}Ga; Somatostatin receptor; [Tyr^3]octreotide; Positron emission tomography; Peptide

Introduction

The overexpression of somatostatin receptors (SSTR) on a variety of human neuroendocrine tumors has led to interest in these as targets for tumor imaging and therapy. The natural ligand for these receptors, somatostatin (SST), was first described in 1973 as a hypothalamic hormone that inhibits secretion of growth hormones [1] and later on found in two physiological forms—SST-14 and SST-28 [2]. While previous studies have shown that both SST-14 and SST-28 may function as different neurotransmitters [3] and have similar

Correspondence to: Suzanne E. Lapi; lapis@mir.wustl.edu.

Conflict of interest. The authors declare no conflict of interest.

binding affinities toward SSTR, the short biological half-life (2–4 min) limits their direct application for developing SSTR-targeted imaging probes [4]. As such, various SST analogs have been designed and characterized.

Among all SST analogs, octreotide and its derivatives have been widely used as imaging agents due to improved biological pharmacokinetics and targeting specificity [5, 6]. ^{111}In-labeled octreotide (^{111}In-OctreoScan; biological half-life, 1.7–1.9 h) was the first SSTR-targeting radiotracer approved for clinical use in the USA [7]. Since then, ^{68}Ga, ^{90}Y, and ^{177}Lu labeled DOTA-[Tyr^3]-octreotide (DOTATOC; DOTA: 1,4,7,10-tetraazacyclododecane-1,4,7,10-tetraacetic acid) have gained significant relevance for positron emission tomography (PET) and peptide receptor radiotherapy [8–10].

To date, ^{68}Ga-DOTATOC-based PET imaging has been used successfully for diagnosis and therapeutic management of SSTR-expressing tumors [11, 12]. However, as the NOTA-Ga (III) complex (NOTA: 1,4,7-triazacyclononane-1,4,7-triacetic acid) is more thermodynamically stable compared to that of DOTA-Ga(III) complex (log $K_{NOTA\text{-}Ga(III)}$=31.0 vs. log $K_{DOTA\text{-}Ga(III)}$=21.3) [13], Eisenwiener et al. have designed and synthesized a NOTA-based scaffold to conjugate targeting molecules for ^{68}Ga-labeling [14].

Recently, Garcia Garayoa et al. proposed that the presence of negative charges may lead to new peptide analogs with improved biodistribution profiles [15]. This hypothesis was initially based on observations from antibodies since electrostatic effects, particularly in radiolabeled human polyclonal antibodies carrying negative charges, influence the biodistribution profile [16] and can reduce hepatic retention [17]. Although the studies performed by Anderson et al. [18] and Garcia Garayoa et al. [15] yielded similar results on peptide conjugates, their findings were generated by using molecules with different chelating systems and varying hydrophilicities. As such, it is of importance to further define the impact of the molecular charge on the overall performance of peptide conjugates.

In this study, we have synthesized a series of [Tyr^3] octreotide conjugates (Fig. 1) and aimed to evaluate the physiological influence of the molecular charge by modifying chelators of the peptide conjugates. As the carboxylates on the NOTA-based scaffolds of the [Tyr^3]octreotide conjugates were in the form of conjugate base (R-COO−) during our biological evaluations, we therefore hypothesized that the addition of varying numbers of carboxylate groups on the NOTA-based scaffolds would increase the overall negative charge of the molecules without significantly changing hydrophilicity. The conjugates were investigated for binding to AR42J rat pancreatic cancer cells, and the ^{68}Ga-labeled conjugates were evaluated for internalization into these cells. The tumor localization and tissue accumulation of the ^{68}Ga-labeled conjugates were also analyzed in mice bearing AR42J xenografts. ^{68}Ga-**1** illustrated improved tumor to background ratios than the other conjugates or ^{68}Ga-DOTATOC.

Materials and Methods

General

The NOTA-based scaffolds were synthesized based on previously published procedures [19, 20]. All reagents and solvents were purchased from Sigma-Aldrich (St. Louis, MO) and used as received unless otherwise noted. Milli-Q water (18 MΩ-cm) was obtained from a Millipore Gradient Milli-Q water system (Billerica, MA). Low adhesion 1.5 ml vials and C_{18} Sep-Pak cartridges were purchased from USA Scientific (Ocala, FL) and Millipore (Billerica, MA), respectively. C_{18} Sep-Pak cartridges were conditioned with ethanol and water (5 ml of each) before use. Nitric acid (10–20 %) used for acid washing was prepared by diluting 70 % nitric acid with Milli-Q water. ^{68}Ga was eluted from IGG100 (Eckert & Ziegler Isotope Products, Berlin, Germany) using 0.1 M HCl. Strata X-C columns were purchased from Phenomenex (Torrance, CA). DOTA-[Tyr^3]octreotide and NO2A-[Tyr^3]octreotide were purchased from CPC Scientific (Sunnyvale, CA). Matrix-assisted laser desorption/ionization time-of-flight (MALDI-TOF) mass spectra (MALDI-MS) were collected on a Voyager-DE™ PRO Biospectrometry Workstation (Applied Biosystems, Foster City, CA).

Preparation of the [Tyr^3]Octreotide Conjugates

The [Tyr^3, Lys(Boc)^5]octreotide conjugation with the NOTA-based scaffolds was achieved by reacting the peptide through a primary amine in the N-terminal D-Phe. The carboxylates glutaric acid 1-tert-butyl ester on the NOTA-based scaffolds (3.3–4.1 mg, 6.0 μmol) were activated by 2-(1H-7-azabenzotriazol-1-yl)-1,1,3,3-tetramethyl uronium hexafluorophosphate (2.3 mg, 6.0 μmol) and then reacted with the peptide (2.3 mg, 2.0 μmol; molar ratio scaffold: peptides=3:1) overnight at room temperature in DMSO. The unreacted scaffolds and peptides were removed by HPLC with a Vydac C_{18} column (5 μm, 4.6×250 mm), followed by lyophilization. After deprotecting with 95 % TFA, the crude [Tyr^3]octreotide conjugates were purified again by HPLC (for both HPLC purifications, the flow rate was set at 1 ml/min using a gradient system starting from 100 % solvent A by a linear ramp to 100 % solvent B at 50 min. Solvent A, 0.1 % trifluoroacetic acid (TFA) in water (*v*/*v*); solvent B, 0.1 % TFA in acetonitrile (*v*/*v*)). Yields of 1.0, 0.5, and 0.3 mg of material was obtained for conjugates 1, 2, and 3, respectively using 2.3 mg (2 μmol) of [Tyr^3, Lys(Boc)^5]octreotide starting material. The conjugates were characterized by MALDI-MS with α-cyano-4-hydroxycinnamic acid (**1** ($C_{49}H_{65}N_{10}O_{11}S_2$): $[MH]^+$ calculated 1,391.59*m*/*z*, found 1,391.99*m*/*z*; **2** ($C_{67}H_{92}N_{13}O_{20}S_2$): $[MH]^+$ calculated 1,463.65, found 1,462.45 ; **3** ($C_{70}H_{96}N_{13}O_{22}S_2$): $[MH]^+$ calculated 1,535.72, found 1,535.78).

Radiochemistry

The ^{68}Ga eluate was purified by a Strata X-C column following the published method [21]. The Strata X-C column contained 30 mg of the cation resin and eliminates the impurities of the ^{68}Ga eluate [21]. The Strata X-C columns were used without preconditioning. The eluate (6–10 ml) was slowly passed through the column (2 ml/min) and the resin was dried with air. The purified ^{68}Ga eluate was obtained by desorbing the activity from the resin with 0.5 ml of 0.02 M HCl/98 % acetone.

For radiolabeling, the purified ^{68}Ga eluate (50 μl, 1.0–1.5 mCi) was added to a 1.5 ml vial containing 1–10 μg of the [Tyr^3] octreotide conjugate in 50 μl of 1 M 4-(2-hydroxyethyl)-1-piperazineethanesulfonic acid (HEPES, pH 4). The reaction mixture was incubated at 95 °C for 10 min in an Eppendorf thermomixer at a constant shaking rate of 1,000 rpm. After addition of diethylenetriamine pentaacetic acid (DTPA, 5 mM, 20 μl) to challenge the nonspecifically bound ^{68}Ga, the labeled peptide was purified by a pre-conditioned C_{18} Sep-Pak cartridge as previously described [21]. HPLC analysis was performed to determine the radiochemical purity of each ^{68}Ga-labeled peptide conjugate.

Determination of Log P Values

The ^{68}Ga-labeled [Tyr^3]octreotide conjugates (20 μl with 5–10 μCi per conjugate) were added into an equal volume mixture of *n*-octanol and Milli-Q water (500 μl/ea). The samples were vortexed at 1,000 rpm for 1 h, followed by removing aliquots of 100 μl from both the aqueous water and the organic *n*-octanol layers and counted separately in a γ counter (Wallac Wizard 3” Automatic Gamma Counter, PerkinElmer, Waltham, MA). The partition coefficients defined as (activity concentration in *n*-octanol)/(activity concentration in aqueous layer) were then calculated to yield log *P* values.

Cell Culture

The AR42J rat pancreatic cancer cell line was purchased from ATCC (Manassas, VA). The cells were maintained in IMDM (Iscove’s Modified Dulbecco's Media) medium with 20 % fetal bovine serum and 0.1 % gentamicin at 37 °C in an atmosphere containing 5 % CO_2.

Internalization Studies

Twenty-four hours prior to the assay, AR42J cells were seeded in six-well plates (1×10^6 cells/well) and allowed to adhere. The cells were rinsed with 10 mM phosphate buffered saline (PBS), followed by addition of the ^{68}Ga-labeled conjugates (~0.7 nM/well; 1 ml/well) in Dulbecco's modified eagle medium (DMEM; containing 0.1 % of bovine serum albumin). Next, the cells were incubated at 37 °C for 10, 30, 60, and 120 min to allow for binding and internalization. After incubation, the cells were washed twice with cold PBS. Surface-bound activity was removed by acid wash (50 mM glycine/HCL, 100 mM NaCl, pH 2.8, 2×1 ml for 5 min at room temperature). Finally, the cells were lysed with 1 N NaOH (2×1 ml). Surface-bound and internalized activities were measured in a γ-counter. The protein concentration was determined using Bio-Rad Protein Assay Kit (Hercules, CA) and results were calculated as percentage of total added radioactivity per 0.1 mg of protein.

Receptor Binding Assays

Somatostatin receptor binding affinities of [Tyr^3]octreotide and the five peptide conjugates were determined by competitive binding assays with ^{68}Ga-DOTATOC as a radioligand. Experiments were performed on 24-well plates seeded with AR42J rat pancreatic tumor cells (5×10^5 cells/well). The cells were rinsed with 10 mM PBS, followed by the addition of ^{68}Ga-DOTATOC solutions (~3.3×10^{-2} nM/well; 0.5 ml/well) mixed with the peptide conjugates at 0–1,000 nM in DMEM (containing 0.1 % of bovine serum albumin). After incubation at 37 °C for 1 h, the cells were rinsed twice with cold PBS and lysed with 1 N

NaOH. The cell lysate was collected and counted by a γ-counter. The cell uptake of ^{68}Ga-DOTATOC was normalized in terms of added radioactivity and protein concentration of the seeded cells. The IC_{50} values were calculated by fitting the quadruplicate data with nonlinear regression using Graph-Pad Prism (GraphPad Software, La Jolla, CA).

Immunofluorescence Microscopy

In vitro fluorescent imaging studies were performed according to a published procedure [22] with slight modifications. Forty-eight hours prior to the studies, AR42J cells were grown on four-well culture slides (2×10^5 cells per chamber) coated with poly-D-lysine (BD Biosciences, San Jose, CA). On the day of the experiment, somatostatin receptor 2 (SSTR2) was labeled by incubating cells for 2 h at room temperature with the rabbit anti-SSTR2 polyclonal antibody (1:100; abcam, Cambridge, MA) diluted in IMDM containing 0.1 % bovine serum albumin (BSA). After removing unbound antibody, cells were washed with PBS and incubated for 30 min at 37 °C with or without [Tyr^3]octreotide conjugates (100 nM per conjugate). Cells were then fixed and permeabilized for 5 min in −20 °C methanol. After washing with PBS, cells were incubated with the goat anti-rabbit Alexa Fluor® 488 antibody (1:600; Life Technologies, Grand Island, NY) in PBS with 0.1 % BSA for 1 h at room temperature. After three additional washes with PBS, the cells were embedded in DAPI Fluoromount G mounting solution (SouthernBiotech, Birmingham, Al). The slides were evaluated and photographed via a ZEISS LSM 510 META laser scanning confocal microscope (LSM TECH, Etters, PA) equipped with a JEOL 1200 EX II transmission electron camera (Technical Sales Solutions, LLC, Beaverton, OR). Images were captured using LSM 510 Examiner (LSM TECH, Etters, PA) acquisition and analysis software.

Biodistribution

All animal studies were performed in compliance with guidelines set forth by the National Institutes of Health Office of Laboratory Animal Welfare and approved by the Washington University Animal Studies Committee. The animal model was established by subcutaneous injection of AR42J cell suspension (5×10^6 cells) into the right flank of male athymic nude mice. When the xenografts reached the size of 50–200 mm^3 (typically 2–3 weeks post subcutaneous injection), the tumor-bearing mice were randomly grouped for the biodistribution studies. During the studies, each mouse was weighed and received 5 μCi of a ^{68}Ga-labeled peptide conjugate via tail vein injection. The mice were anesthetized and sacrificed at 30 min, 1 h, and 2 h p.i. (n=4). Blood, lung, liver, spleen, kidney, muscle, fat, heart, pancreas, stomach, and tumor were collected, weighed, and counted by a γ-counter. The percentage of injected dose per gram (%ID/g) for each sample and the standard deviation (SD) for each group of the organ were determined by comparing the standards (n=3) prepared along with the injection doses.

Statistical Analysis

Quantitative data were processed by Prism 5 (GraphPad Software, La Jolla, CA) and expressed as mean ± SD. All analyses were performed by one-way analysis of variance and Student's t test. P values <0.05 were considered statistically significant.

Results

Radiochemistry

The ^{68}Ga labeling efficiencies were evaluated at 95 °C for all conjugates by varying the concentrations of the conjugates. At the non-carrier-added level, 1 μg of all peptide conjugates in 50 μl of 1 M HEPES (pH 4) were successfully labeled with ^{68}Ga with high labeling efficiencies (>80 %). The ^{68}Ga-labeled conjugates were purified in one step using a pre-activated C_{18} Sep-Pak light cartridge with a >75 % recovery rate. The radiochemical purity of the labeled peptide conjugates post purification by C_{18} Sep-Pak cartridge was >95 % as determined by HPLC. The overall radiochemical procedure took 20 min with resulting specific activities of ~48 GBq/μmol (1.3 Ci/μmol).

Determination of Log P Values

As shown in Table 1, all of the ^{68}Ga-labeled peptide conjugates have similar hydrophilic characteristics with log *P* values less than −2.3. This indicates the incorporation of additional carboxylate groups or negative charges did not result in a clear increase or decrease of hydrophilicity for the peptide conjugates.

Internalization Studies

Rapid internalization of ^{68}Ga-DOTATOC as the reference peptide conjugate was observed throughout the studies (Fig. 2). Internalization of ^{68}Ga-**1** (three carboxylates) was slightly higher than that of the reference peptide at all timepoints. However, internalization of ^{68}Ga-NO2ATOC (two carboxylates) and ^{68}Ga-**2** (four carboxylates) was significantly decreased and that of ^{68}Ga-**3** (five carboxylates) was negligible. These results suggest that the chelator with the same core but various number of carboxylate groups has a significant impact on the internalization.

Receptor Binding Assays

The *in vitro* SSTR binding affinities of the [Tyr^3]octreotide and its conjugates were determined by a competitive cell binding assays using ^{68}Ga-DOTATOC as the SSTR-specific radioligand. In this study, the binding affinity was tested for the unlabeled conjugates. [Tyr^3]octreotide and its conjugates inhibited the binding of ^{68}Ga-DOTATOC to the SSTR overexpressing cells in a dose-dependent manner. Calculated IC_{50} values of the DOTATOC, NO2ATOC, conjugates **1**, **2**, and **3** were determined to be 8.82±3.28, 37.49±15.13, 14.09±0.75, 33.66±2.86, and 125.4±48.0 nM, respectively. The binding affinities of these peptide conjugates were significantly different ($P<0.05$) to that of [Tyr^3]octreotide (3.45±1.11 nM), indicating that the conjugation of a chelating moiety to [Tyr^3]octreotide has a profound effect on the receptor binding affinity of the [Tyr^3]octreotide conjugates. In addition, our findings also suggest that the increased number of carboxylates on the chelator of the same core can result in a reduced binding affinity.

Immunofluorescence Microscopy

Previous reports indicate that AR42J cells express SSTR1, 2, and 3 [22]. As octreotide analogs usually show higher binding affinities toward SSTR2 [20], we chose this receptor as

the model biomarker and determined the effect of chelator modifications in the [Tyr^3]octreotide conjugates on SSTR2 endocytosis. The results in Fig. 3 demonstrate that all conjugates induced receptor endocytosis in AR42J cells with DOTATOC triggering much higher SSTR2 internalization than the other conjugates.

Biodistribution

The tissue distribution profiles of ^{68}Ga-DOTATOC, ^{68}Ga-NO2ATOC, ^{68}Ga-**1**, ^{68}Ga-**2**, and ^{68}Ga-**3** in male athymic nude mice bearing SSTR-positive AR42J tumors are summarized in Fig. 4. Among the organs evaluated, the kidney showed the highest uptake at 30 min p.i. (^{68}Ga-DOTATOC, 11.33±2.07 %ID/g; ^{68}Ga-NO2ATOC, 14.25±2.07 %ID/g; ^{68}Ga-**1**, 22.81±2.22 %ID/g; ^{68}Ga-**2**, 18.20±1.84 %ID/g; ^{68}Ga-**3**, 13.78±2.22 %ID/g), indicating that all the peptide conjugates were primarily excreted from the renal system. At 2 h p.i., while less than 52 % of the initial kidney uptake was retained for ^{68}Ga-NO2ATOC (7.40±1.09 %ID/g), ^{68}Ga-**1** (9.79±1.90 %ID/g), ^{68}Ga-**2** (8.22±2.29 %ID/g), and ^{68}Ga-**3** (5.24±1.03 %ID/g), and ^{68}Ga-DOTATOC (7.33±1.28 %ID/g) showed around 65 % retention. No significant difference was observed for the liver uptake of the peptide conjugates at 30 min p.i. (^{68}Ga-DOTATOC, 0.74±0.18 %ID/g; ^{68}Ga-NO2ATOC, 0.88±0.33 %ID/g; ^{68}Ga-**1**, 0.81±0.09 %ID/g; ^{68}Ga-**2**, 1.38±0.11 %ID/g; ^{68}Ga-**3**, 0.51±0.05 %ID/g). However, the liver uptake of ^{68}Ga-DOTATOC was dramatically increased at 2 h p.i. (4.37±0.20 %ID/g). These findings might be explained by different chelating systems which lead to the altered renal and hepatic retentions.

The tumor uptake of the peptide conjugates showed a positive correlation with the *in vitro* internalization results at 1 h p.i. (^{68}Ga-DOTATOC, 13.49±6.28 %ID/g; ^{68}Ga-NO2ATOC, 9.15±3.01 %ID/g; ^{68}Ga-**1**, 22.31±3.22 %ID/g; ^{68}Ga-**2**, 7.87±0.41 %ID/g; ^{68}Ga-**3**, 2.95±0.62 %ID/g). However, whereas there was no significant change of the tumor uptake for ^{68}Ga-DOTATOC and ^{68}Ga-NO2ATOC throughout the studies, the tumor uptake for ^{68}Ga-**1**, ^{68}Ga-**2**, and ^{68}Ga-**3** was somewhat reduced at 2 h p.i. (^{68}Ga-**1**, 12.82±4.65 %ID/g; ^{68}Ga-**2**, 1.78±0.15 %ID/g; ^{68}Ga-**3**, 0.83±0.10 %ID/g) indicating some washout of these compounds. The tumor retention rate of ^{68}Ga-**1**, ^{68}Ga-**2**, and ^{68}Ga-**3** at 2 h p.i. was on the order of ^{68}Ga-**1** (55 %)>^{68}Ga-**2** (24 %)>^{68}Ga-**3** (19 %).

The tumor/lung, tumor/liver, tumor/kidney, tumor/pancreas, and tumor/stomach ratios for the peptide conjugates at 1 h p.i. are shown in Fig. 5. Although ^{68}Ga-**3** generally had lower normal tissue uptake than the other peptide conjugates, the tumor uptake was also lower and thus tumor/normal tissue ratios are similar to ^{68}Ga-DOTATOC and ^{68}Ga-NO2ATOC. An exception to this is the tumor/stomach ratios. ^{68}Ga-**3** had a significantly higher (P<0.01) tumor/stomach ratio at 1 h p.i. than that of ^{68}Ga-DOTATOC, ^{68}Ga-NO2ATOC, and ^{68}Ga-**2**. Both ^{68}Ga-DOTATOC and ^{68}Ga-**1** had significantly higher (P<0.05) tumor/liver and tumor/kidney ratios than those of ^{68}Ga-**2** and ^{68}Ga-**3** at 1 h. In general, ^{68}Ga-**1** was somewhat superior overall in terms of the liver, kidney, and stomach ratios.

Discussion

Due to the potential for the detection and therapy of SSTR-expressing tumors, a variety of octreotide analogs have been labeled with different radionuclides for the past decade.

However, interest in using ^{68}Ga-labeled octreotide analogs for clinical PET applications dramatically increased after Henze et al. reported the promising imaging results of ^{68}Ga-DOTATOC in patients with SSTR-overexpressed meningiomas [23]. As the availability of ^{68}Ga from a ^{68}Ge/^{68}Ga generator eliminates the need of an onsite cyclotron, and fully automated systems for synthesizing ^{68}Ga-labeled peptides have become commercially available [21], ^{68}Ga-labeled octreotide analogs have recently gained significant attention for their potential in diagnosing and managing neuroendocrine tumors [24–27].

Our work aimed to evaluate the physiological influence of chelator modifications on the peptide imaging agents *in vitro* and *in vivo*. In order to investigate this, we have used [Tyr^3]octreotide as a model peptide system and conjugated this structure with the NOTA-based scaffolds having two to five copies of carboxylate groups. All peptide conjugates studied herein had similar partition coefficients and hydrophilicities. As the chemical structures of the pendent arms on the NOTA-based scaffolds are similar to those of acetic acid or succinic acid, their logarithmic acid dissociation constant [28] is well below 6 [29]. Considering all of our biological evaluations were performed in the cultured cells and laboratory mice, the carboxylates of the NOTA-based scaffolds are believed to be persisted as the conjugate base (R-COO−) (the pH value of the blood in the laboratory mouse is 7.3–7.4 [30]). In this regard, our studies allowed us for a more precise evaluation of the effects of molecular charge on the [Tyr^3]octreotide conjugates.

In vitro internalization studies in the AR42J rat pancreatic cancer cells reflected an agonistic behavior for the all peptide conjugates. This finding was consistent with the data previously reported for the other octreotide analog conjugates labeled by different radionuclides [14, 31, 32]. The internalization of the ^{68}Ga-labeled conjugate **1** (three carboxylates) was comparable to that of ^{68}Ga-DOTATOC (three carboxylates) although some discrepancy appears when comparing the radioactive internalization studies with the microscopy. The reason for this is not clear although it may be that the DOTATOC is washed out in the radiotracer internalization studies whereas the confocal images are showing the receptor itself (which remains inside the cell), rather than the compound. This is supported by the biodistribution data. This may also be partially due to effects of other somatostatin receptors in the radioactive internalization studies, whereas the confocal images only show SSTR2. However, the internalization of ^{68}Ga-labeled NO2ATOC (two carboxylates) and the conjugates **2** (four carboxylates) and **3** (five carboxylates) was significantly reduced. Considering the major compositions (e.g. phospholipids, glycoproteins) that lead to cell membranes with negative charges, it is somewhat surprising that ^{68}Ga-NO2ATOC had poor cellular internalization. As the coordination number of Ga(III) can be either 4 or 6 [13] and Ga (III)-NO2ATOC is the only peptide conjugate with the possible coordination number of 4, this phenomenon might be explained by different coordinating systems that lead to the altered properties. Indeed, the stimulation of SSTR2 internalization by NO2ATOC was significantly lower than that of DOTATOC. Furthermore, we found that the increased number of carboxylates on the chelator of the same core seems to further reduce SSTR2 internalization and overall SSTR binding affinities. With these regards, we believe that the coordinating and chelating systems have a strong influence on the cellular internalization of the ^{68}Ga-labeled [Tyr^3]octreotide conjugates.

Our biodistribution study shows that ^{68}Ga-**1** has the highest tumor uptake at 1 h p.i. compared to the other peptide conjugates. Unlike the biodistribution data of ^{68}Ga-labeled DOTATOC and NO2ATOC, this peptide conjugate showed some washout from the tumor but still maintained the same or higher tumor accumulation at later timepoints. This washout has also been noticed by Eisenwiener et al. during biodistribution studies of ^{67}Ga-labeled NODAGATOC (^{67}Ga-**1**; the half-life of ^{67}Ga is 3.26 days) and DOTATOC on AR42J tumor-bearing mice [20]. Of the normal tissues, our [Tyr^3]octreotide conjugates predominately accumulated in the kidney. In addition to the fact that these peptide conjugates were primarily excreted from the renal system, they might be below the renal filtration limit and reabsorbed in the proximal tubular cells [33, 34]. In fact, Vegt et al. were able to reduce the kidney uptake of ^{111}In-labeled DTPA-octreotide by co-injecting albumin fragments or albumin-derived peptides [35, 36]. The kidney washout of ^{68}Ga-**1**, ^{68}Ga-**2**, and ^{68}Ga-**3** was significantly altered with the number of carboxylates on the NOTA-based chelators. However, the kidney uptake of ^{68}Ga-DOTATOC (three carboxylates) and ^{68}Ga-NO2ATOC (two carboxylates) was significantly lower than that of ^{68}Ga-**1** and ^{68}Ga-**2** at 30 min and 1 h p.i. Thus, the number of carboxylates in the chelator of peptide conjugates and the selection of radiometal chelating systems may lead to altered biodistribution profiles. Also of interest is the increased liver signal obtained with ^{68}Ga-DOTATOC at 2 h. p.i. Although further investigations are needed, lower stability of the DOTA-Ga(III) complex ($\log K_{NOTA\text{-}Ga(III)}$=31.0 vs. $\log K_{DOTA\text{-}Ga(III)}$=21.3) [13] could be one of the possible causes for this observation.

Conclusion

In this study, we evaluated four ^{68}Ga-labeled [Tyr^3] octreotide conjugates that consisted of different NOTA-based chelators with two to five copies of carboxylates and compared our results with ^{68}Ga-DOTATOC. Among all of the peptide conjugates, ^{68}Ga-**1** showed a preferable biodistribution profile that was comparable to or better than that of ^{68}Ga-DOTATOC, while the addition of further carboxylate groups led to unfavorable biodistribution profiles. Our findings suggest that the chelator modifications and the selection of radiometal chelating systems can lead to altered pharmacokinetics.

Acknowledgments

The authors were saddened by the loss of Dr. Michael J. Welch on May 6, 2012. Nicole Fettig, Margaret Morris, Amanda Roth, and Lori Strong are thanked for performing the biodistribution studies. This work was supported by DOE Integrated Research Training Program of Excellence in Radiochemistry (DE-SC0002032).

References

1. Brazeau P, Vale W, Burgus R, et al. Hypothalamic polypeptide that inhibits the secretion of immunoreactive pituitary growth hormone. Science. 1973; 179:77–79. [PubMed: 4682131]
2. Reichlin S. Somatostatin. N Engl J Med. 1983; 309:1495–1501. [PubMed: 6139753]
3. Wang HL, Bogen C, Reisine T, Dichter M. Somatostatin-14 and somatostatin-28 induce opposite effects on potassium currents in rat neocortical neurons. Proc Natl Acad Sci U S A. 1989; 86:9616–9620. [PubMed: 2574465]

4. Bal CS, Gupta SK, Zaknun JJ. Radiolabeled somatostatin analogs for radionuclide imaging and therapy in patients with gastroenteropancreatic neuroendocrine tumors. Trop Gastroenterol. 2010; 31:87–95. [PubMed: 20862981]
5. Pawlikowski M, Melen-Mucha G. Somatostatin analogs—from new molecules to new applications. Curr Opin Pharmacol. 2004; 4:608–613. [PubMed: 15525552]
6. Pool SE, Krenning EP, Koning GA, et al. Preclinical and clinical studies of peptide receptor radionuclide therapy. Semin Nucl Med. 2010; 40:209–218. [PubMed: 20350630]
7. Breeman WA, de Jong M, Kwekkeboom DJ, et al. Somatostatin receptor-mediated imaging and therapy: basic science, current knowledge, limitations and future perspectives. Eur J Nucl Med. 2001; 28:1421–1429. [PubMed: 11585303]
8. Maecke HR, Hofmann M, Haberkorn U. (68)Ga-labeled peptides in tumor imaging. J Nucl Med. 2005; 46(Suppl 1):172S–178S. [PubMed: 15653666]
9. Kwekkeboom DJ, Mueller-Brand J, Paganelli G, et al. Overview of results of peptide receptor radionuclide therapy with 3 radiolabeled somatostatin analogs. J Nucl Med. 2005; 46(Suppl 1):62S–66S. [PubMed: 15653653]
10. Kwekkeboom DJ, Bakker WH, Kooij PP, et al. [^{177}Lu-DOTAOTyr^{3}]octreotate: comparison with [^{111}In-DTPAo]octreotide in patients. Eur J Nucl Med. 2001; 28:1319–1325. [PubMed: 11585290]
11. Ruf J, Heuck F, Schiefer J, et al. Impact of multiphase ^{68}Ga-DOTATOC-PET/CT on therapy management in patients with neuroendocrine tumors. Neuroendocrinology. 2010; 91:101–109. [PubMed: 19996582]
12. Putzer D, Gabriel M, Henninger B, et al. Bone metastases in patients with neuroendocrine tumor: ^{68}Ga-DOTA-Tyr^{3}-octreotide PET in comparison to CT and bone scintigraphy. J Nucl Med. 2009; 50:1214–1221. [PubMed: 19617343]
13. Wadas TJ, Wong EH, Weisman GR, Anderson CJ. Coordinating radiometals of copper, gallium, indium, yttrium, and zirconium for PET and SPECT imaging of disease. Chem Rev. 2010; 110:2858–2902. [PubMed: 20415480]
14. Eisenwiener KP, Prata MI, Buschmann I, et al. NODAGATOC, a new chelator-coupled somatostatin analogue labeled with [$^{67/68}$Ga] and [^{111}In] for SPECT, PET, and targeted therapeutic applications of somatostatin receptor (hsst2) expressing tumors. Bioconjug Chem. 2002; 13:530–541. [PubMed: 12009943]
15. Garcia Garayoa E, Schweinsberg C, Maes V, et al. Influence of the molecular charge on the biodistribution of bombesin analogues labeled with the [99mTc(CO)$_3$]-core. Bioconjug Chem. 2008; 19:2409–2416. [PubMed: 18998719]
16. ten Kate CI, Fischman AJ, Rubin RH, et al. Effect of isoelectric point on biodistribution and inflammation: imaging with indium-^{111}-labelled IgG. Eur J Nucl Med. 1990; 17:305–309. [PubMed: 2286203]
17. Khaw BA, Klibanov A, O'Donnell SM, et al. Gamma imaging with negatively charge-modified monoclonal antibody: modification with synthetic polymers. J Nucl Med. 1991; 32:1742–1751. [PubMed: 1880577]
18. Anderson CJ, Pajeau TS, Edwards WB, Sherman EL, Rogers BE, Welch MJ. *In vitro* and *in vivo* evaluation of copper-64-octreotide conjugates. J Nucl Med. 1995; 36:2315–2325. [PubMed: 8523125]
19. Sun X, Singh AN. Multivalent bifunctional chelator scaffolds for gallium-68 based positron emission tomography imaging probe design: signal amplification via multivalency. Bioconjug Chem. 2011; 22(8):1650–1662. [PubMed: 21740059]
20. Eisenwiener K-P, Prata MIM, Buschmann I, et al. NODAGATOC, a new chelator-coupled somatostatin analogue labeled with [$^{67/68}$Ga] and [^{111}In] for SPECT, PET, and targeted therapeutic applications of somatostatin receptor (hsst2) expressing tumors. Bioconjug Chem. 2002; 13:530–541. [PubMed: 12009943]
21. Lin M, Ranganathan D, Mori T, et al. Long-term evaluation of TiO(2)-based (68)Ge/(68)Ga generators and optimized automation of [(68)Ga]DOTATOC radiosynthesis. Appl Rad Isot. 2012; 70:2539–2544.

22. Liu Q, Cescato R, Dewi DA, Rivier J, Reubi JC, Schonbrunn A. Receptor signaling and endocytosis are differentially regulated by somatostatin analogs. Mol Pharmacol. 2005; 68:90–101. [PubMed: 15855408]
23. Henze M, Schuhmacher J, Hipp P, et al. PET imaging of somatostatin receptors using [^{68}GA]DOTA-D-Phe^{1}-Tyr^{3}-octreotide: first results in patients with meningiomas. J Nucl Med. 2001; 42:1053–1056. [PubMed: 11438627]
24. Hofman MS, Kong G, Neels OC, Eu P, Hong E, Hicks RJ. High management impact of Ga-68 DOTATATE (GaTate) PET/CT for imaging neuroendocrine and other somatostatin expressing tumours. J Med imaging Radiat Oncol. 2012; 56:40–47. [PubMed: 22339744]
25. Naswa N, Karunanithi S, Soundararajan R, et al. Metastatic neuroendocrine carcinoma presenting as a "Superscan" on ^{68}Ga-DOTANOC somatostatin receptor PET/CT. Clin Nucl Med. 2012; 37:892–894. [PubMed: 22889781]
26. Naji M, AL-N A. (6)(8)Ga-labelled peptides in the management of neuroectodermal tumours. Eur J NuclMedMol Imaging. 2012; 39(Suppl 1):S61–S67.
27. Ambrosini V, Campana D, Tomassetti P, Fanti S. (6)(8)G-alabelled peptides for diagnosis of gastroenteropancreatic NET. Eur J Nucl Med Mol Imaging. 2012; 39(Suppl 1):S52–S60. [PubMed: 22388622]
28. Wagner S, Breyholz HJ, Holtke C, et al. A new ^{18}F-labelled derivative of the MMP inhibitor CGS 27023A for PET: radiosynthesis and initial small-animal PET studies. Appl Radiat Isot. 2009; 67:606–610. [PubMed: 19167232]
29. Dawson, RMC.; Elliott, DC.; Elliott, WH. Data for Biochemical Research. 3rd ed.. Clarendon, New York: 1989.
30. Sprague JE, Li WP, Liang K, Achilefu S, Anderson CJ. *In vitro* and *in vivo* investigation of matrix metalloproteinase expression in metastatic tumor models. Nucl Med Biol. 2006; 33:227–237. [PubMed: 16546677]
31. Decristoforo C, Melendez-Alafort L, Sosabowski JK, Mather SJ. 99mTc-HYNIC-[Tyr^{3}]-octreotide for imaging somatostatin-receptor-positive tumors: preclinical evaluation and comparison with ^{111}Inoctreotide. J Nucl Med. 2000; 41:1114–1119. [PubMed: 10855644]
32. Verwijnen SM, Sillevis Smith PA, Hoeben RC, et al. Molecular imaging and treatment of malignant gliomas following adenoviral transfer of the herpes simplex virus-thymidine kinase gene and the somatostatin receptor subtype 2 gene. Cancer Biother Radiopharm. 2004; 19:111–120. [PubMed: 15068619]
33. Silbernagl S. The renal handling of amino acids and oligopeptides. Physiol Rev. 1988; 68:911–1007. [PubMed: 3293095]
34. Christensen EI, Gburek J. Protein reabsorption in renal proximal tubule-function and dysfunction in kidney pathophysiology. Pediatr Nephrol (Berlin, Germany). 2004; 19:714–721.
35. Vegt E, Eek A, Oyen WJ, de Jong M, Gotthardt M, Boerman OC. Albumin-derived peptides efficiently reduce renal uptake of radiolabelled peptides. Eur J Nucl Med Mol Imaging. 2010; 37(2):226–234. [PubMed: 19722105]
36. Vegt E, van Eerd JE, Eek A, et al. Reducing renal uptake of radiolabeled peptides using albumin fragments. J Nucl Med. 2008; 49:1506–1511. [PubMed: 18703613]

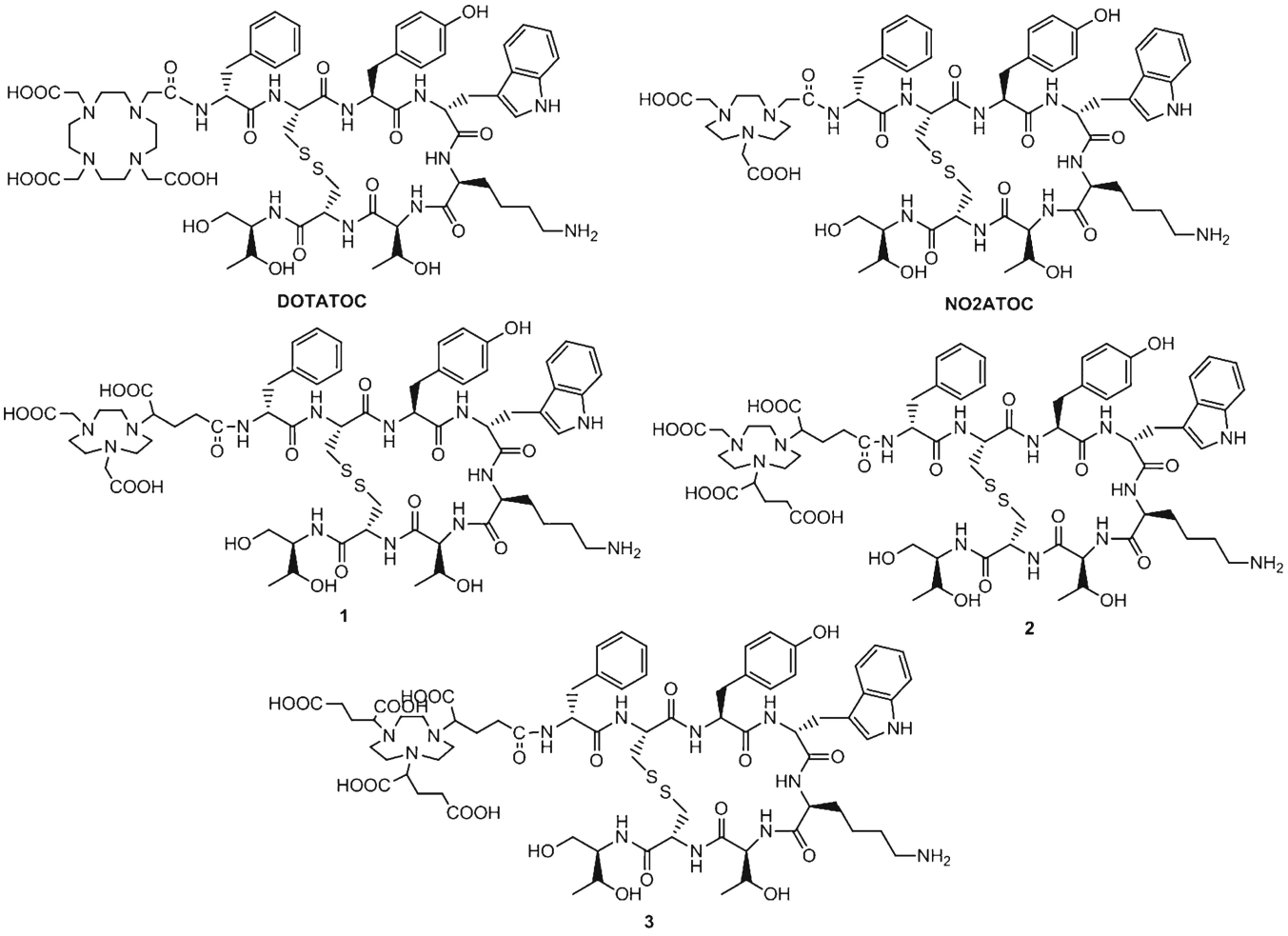

Fig. 1.

Chemical structures of the [Tyr^3]octreotide conjugates: DOTATOC, NO2ATOC, and conjugates **1**, **2**, and **3**.

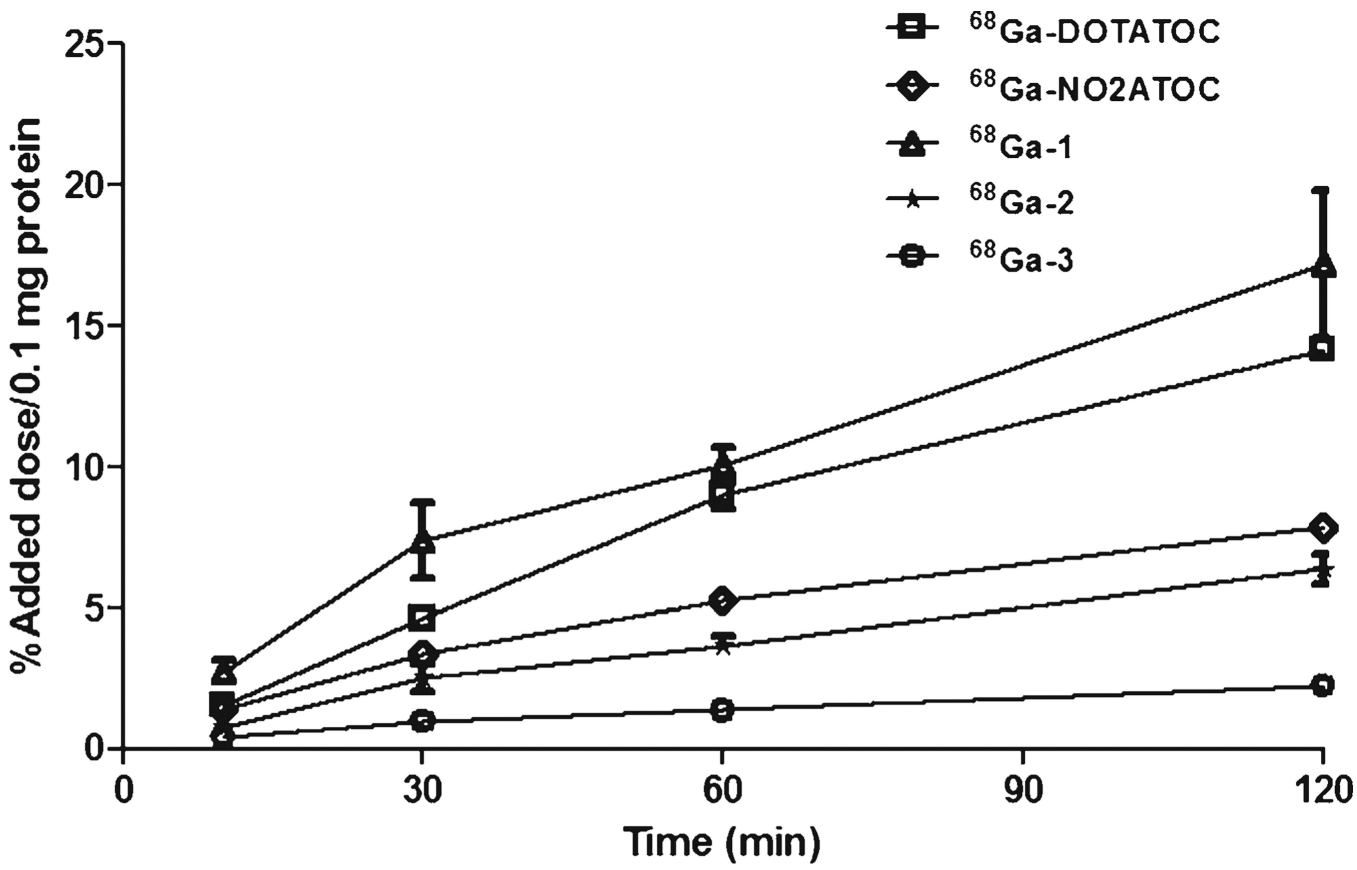

Fig. 2.

Time-course internalization of the ^{68}Ga-labeled [Tyr^3] octreotide conjugates in AR42J cells after incubation at 37 °C. Data represent the percentage of the internalized activity per 100 μg protein related to the total activity added to the cells (*n*=4).

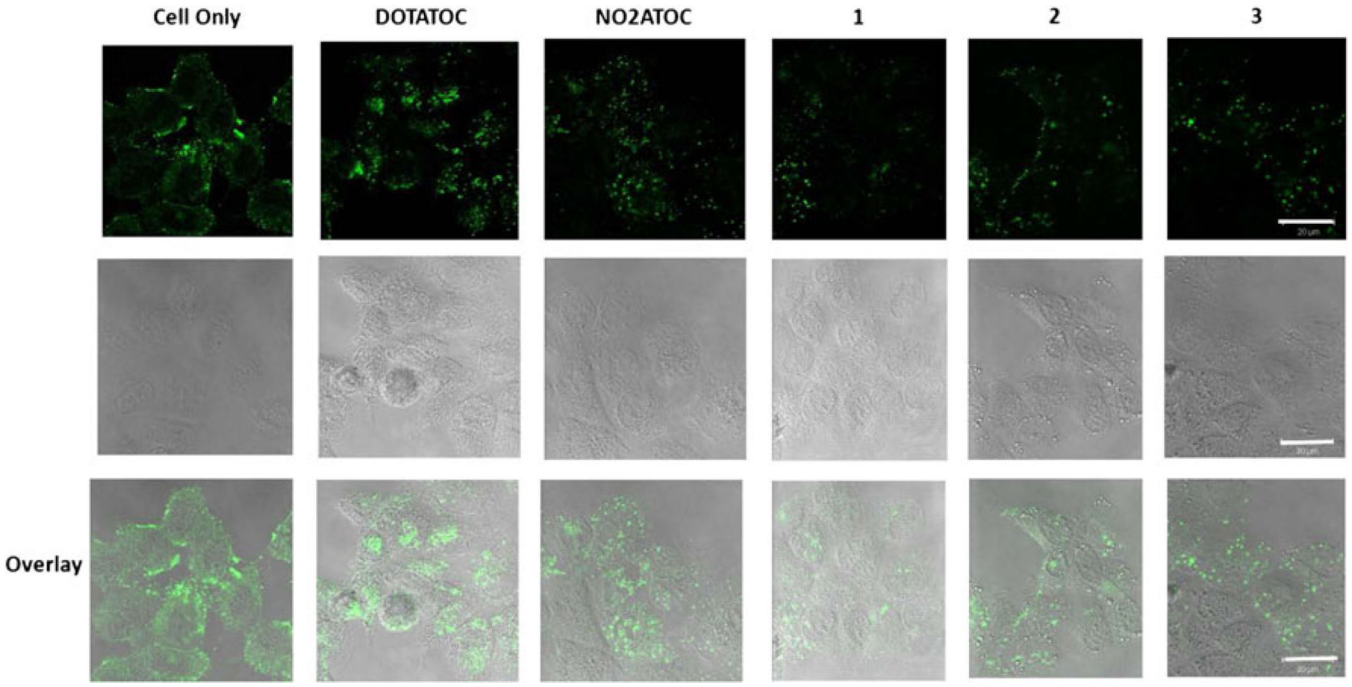

Fig. 3.

Imaging of the internalized SSTR2 induced by the [Tyr^3]octreotide conjugates. Cells were incubated for 30 min at 37 °C with 100 nM of the conjugates. The cells were then processed for immunocytochemistry. The *scale bar* represents a length of 20 μm.

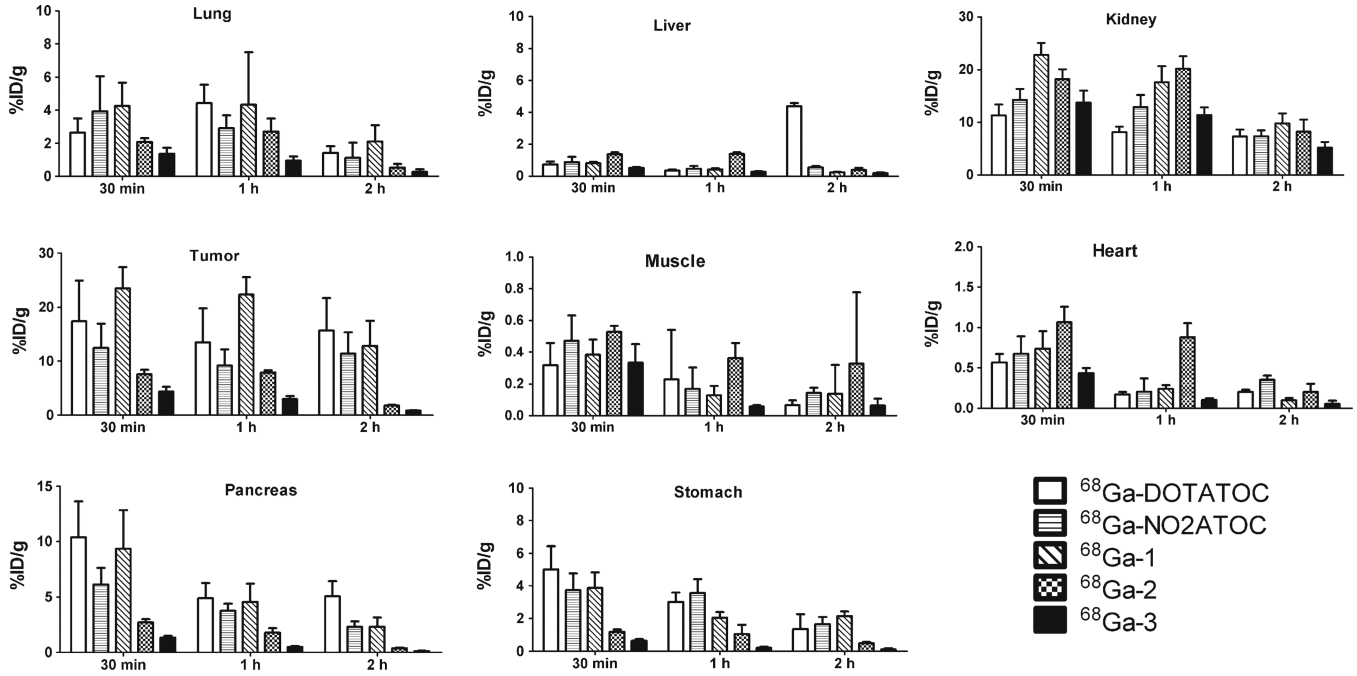

Fig. 4.

Biodistribution profiles of ^{68}Ga-DOTATOC, ^{68}Ga-NO2ATOC, ^{68}Ga-**1**, ^{68}Ga-**2**, ^{68}Ga-**3** in AR42J tumor bearing athymic nude mice at 30 min and 1 and 2 h p.i. Data are presented as %ID/g±SD (*n*=4).

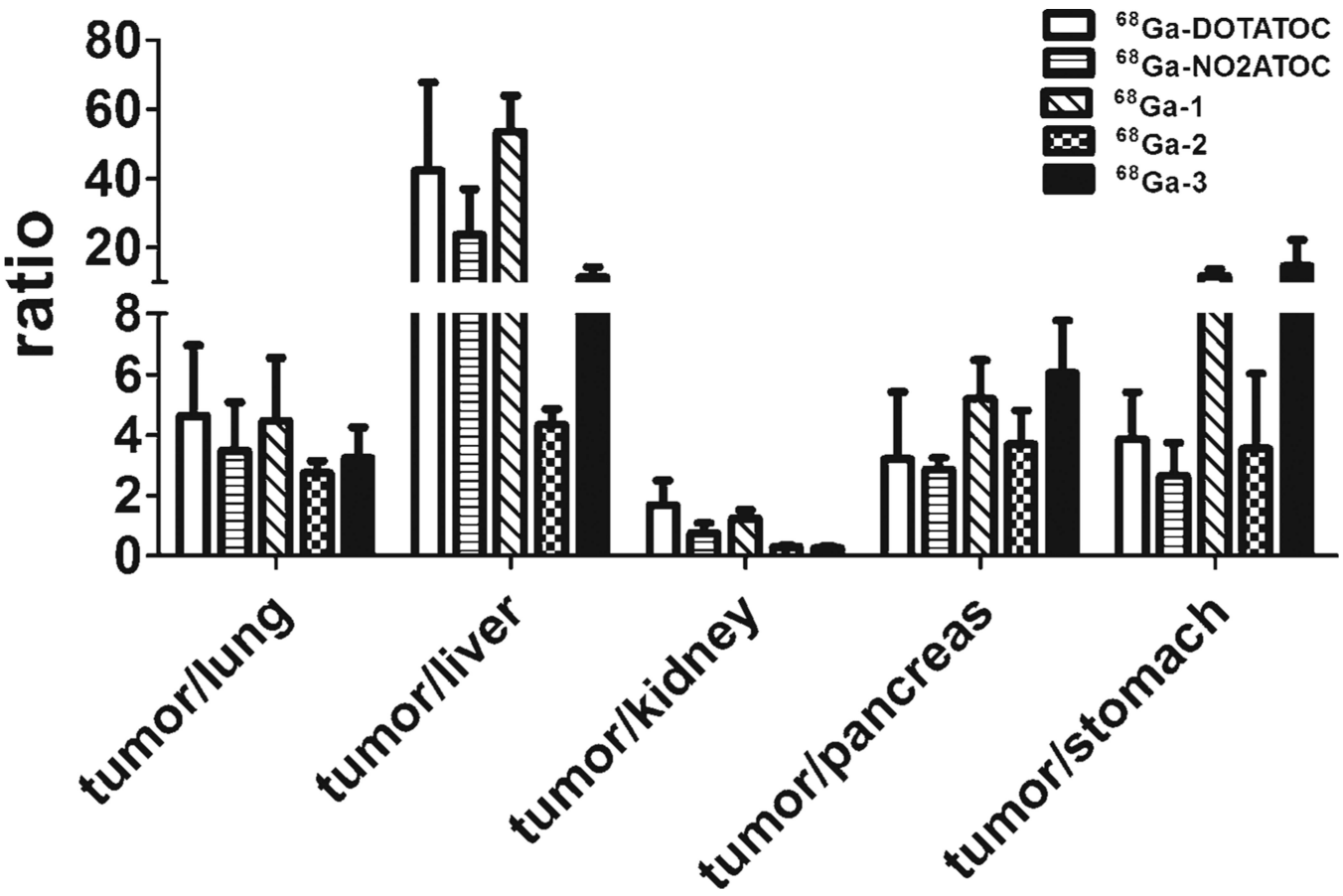

Fig. 5.

Comparative ratios of the tumor uptake to major organs for the ^{68}Ga-labeled [Tyr^3]octreotide conjugates at 1 h p.i.

Table 1

Characteristics of the ^{68}Ga-labeled [Tyr^3]octreotide conjugates

	Copies of carboxylate on the chelator	Retention time (min) analyzed by HPLC	Log *P*
^{68}Ga-DOTATOC	3	16.5	−2.93±0.37
^{68}Ga-NO2ATOC	2	16.9	−2.89±0.19
^{68}Ga-**1**	3	17.0	−2.49±0.19
^{68}Ga-**2**	4	17.3	−2.33±0.09
^{68}Ga-**3**	5	17.5	−2.66 ±0.15